NOTATION

$O\underline{Z}$, direction of the station axis; OX, OY, directions perpendicular to the station axis; g, acceleration vector; g, absolute value of the acceleration vector; ω, angular velocity of rotation of the acceleration vector; ω^*, scaling angular velocity; g^*, scaling absolute value of the acceleration vector; Gr, Grashof number, $Gr = g^*\beta_t\Delta TR^3/\nu^2$; Pr, Prandtl number, $Pr = \nu/a$; ν, kinematic viscosity coefficient; a, coefficient of thermal diffusivity; T, temperature; β_{th}, thermal expansion coefficient; R, characteristic size, radius of the vessel; Ωu, relative angular velocity; Fo, dimensionless time; ψ_m, maximal value of the stream function; ψ_n, relative flow intensity; Gr_C, concentration Grashof number; C, concentration.

LITERATURE CITED

1. S. D. Grishin, V. B. Dubovskoi, S. S. Obydennikov, and V. V. Savichev, in: Technological Experiments in Weightlessness [in Russian] (1983), pp. 6-14.
2. V. S. Avduevskii, A. V. Korol'kov, V. S. Kuptsova, and V. V. Savichev, Zh. Prikl. Mekh. Tekh. Fiz., No. 1, 54-59 (1987).
3. A. M. Vetoshkin, A. V. Korol'kov, V. S. Kuptsova, and V. V. Savichev, Kosm. Nauka Tekh., No. 4, 53-57 (1989).
4. A. V. Korol'kov and V. S. Kuptsova, Chisl. Metod. Mekh. Splosh. Sred., 16, No. 2, 88-95 (1985).

INFLUENCE OF THE ENERGY SUPPLY ON THE CONDITIONS OF SUPERSONIC FLOW AROUND AN OBSTACLE

V. Yu. Borzov, I. V. Rybka, and A. S. Yur'ev

UDC 533.6.011.51

Supersonic flow around an obstacle is calculated in the case of axial nonuniformity of the gasdynamic parameters due to energy supply to the gas in a region upstream from the obstacle. The influence of the distance between the energy-supply region and the obstacle and their relative transverse dimensions on the flow conditions and the lateral-drag coefficient is analyzed.

In practice, it is often necessary to deal with nonuniform supersonic gas flow around a body. Such nonuniformity of the incoming flux may be due to various factors, for example, the formation of a wake behind a body positioned upstream at the pivot of a disk attachment [1], energy and mass supply [2], etc. The character of the nonuniformity depends to a considerable extent on the factors which cause it, and has a significant influence on the flow conditions around an obstacle and the corresponding force and energy interaction.

The flow of nonuniform supersonic flow around an obstacle has recently been studied for the case of energy supply to a local region of the flow [3, 4]. In [3], it was shown that, if a cylindrical body is downstream from a thin thermal layer with reduced density at its axis, approximately threefold reduction in lateral drag is possible, and it was suggested that nonsteady flow conditions are possible here, in principle. The model proposed for the nonuniformity of the incoming flow permits the study of the mechanism of flow restructuring in the shock layer. In practice, however, it is difficult to create a thin thermal layer with constant parameters over its length in a gas, by any known means, since not only radial but also longitudinal nonuniformity of the gasdynamic parameters appears in real conditions. This corresponds to the problem in [4], where supersonic flow around a sphere was calculated in the case of energy input to the flow, with variation in the rate of energy supply and in the distance between the sphere and the region of energy supply. Once again, considerable reduction in the lateral-drag coefficient was found in the calculations.

Translated from Inzhenerno-fizicheskii Zhurnal, Vol. 62, No. 2, pp. 243-247, February, 1992. Original article submitted April 10, 1991.

1062-0125/92/6202-0178$12.50

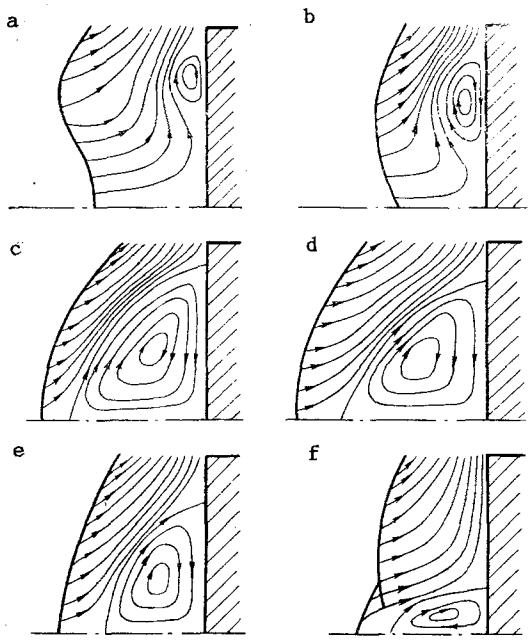

Fig. 1

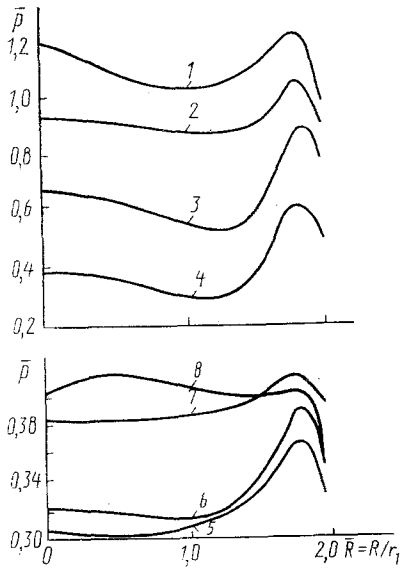

Fig. 2

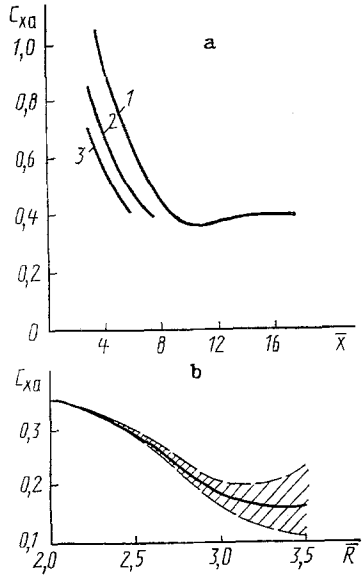

Fig. 3

Fig. 1. Gas flow in shock layer with various distances $\bar{X}$ of the end ($\bar{R}$ = 2.0) from the energy-supply region: a) $\bar{X}$ = 4.1; b) 5.8; c) 8.3; d) 9.1; e) 11.9; f) 13.5.

Fig. 2. Distribution of pressure coefficient $\bar{P}$ over the radius of the end ($\bar{R}$ = 2.0) at different distances from the energy-supply region: 1) $\bar{X}$ = 3.2; 2) 4.1; 3) 5.8; 4) 8.3; 5) 9.1; 6) 10.2; 7) 11.9; 8) 13.5.

Fig. 3. Dependence of the lateral-drag coefficient of the obstacle C_{xa} on $\bar{X}$ (a) when $\bar{R}$ = 2.0 (1), 1.5 (2), and 1.0 (3) and on $\bar{R}$ when $\bar{X}$ = 9.1 (b).

Thus, by appropriate choice of the energy supplied to it, an incoming flux may be deliberately restructured so as to improve the flow around an obstacle (for example, to reduce the lateral resistance of bodies in a gas flow). This possibility is of practical interest, but its realization requires more detailed study of the factors influencing the restructuring of the incoming flow and the flow conditions around the obstacle: primarily, the shape of

the obstacle, the relative position of the energy-supply region and the obstacle, and the ratio of their geometric dimensions.

The present work outlines the results of numerical modeling of an axisymmetric supersonic gas flow around a cylindrical obstacle (radius R) with a plane front end, in the case of strong axial nonuniformity of the flow due to energy supply in a cylindrical region (radius r_1) which is located upstream on the axis. A cylindrical obstacle is chosen so as to reveal more clearly the effects due to nonuniformity of the gasdynamic parameters of the flow.

The influence of the distance from the obstacle to the energy-supply region and the ratio of their transverse dimensions on the shockwave structures formed and the lateral-drag coefficient of the obstacle is investigated, in a two-stage calculation. In the first stage, the field of gasdynamic parameters is determined in the case of energy supply to an unperturbed supersonic flow with $M_\infty = 10$ in a local region. Note that, with a specific power supply $Q = 3 \cdot 10^9$ W/kg, the flow is supersonic in the whole calculation region. This means that, in investigating the influence of the energy supply on the flow around the obstacle, a standard rectangular calculation region (10 × 6) with a fixed position of the obstacle may be used; to take account of the change in the distance between the obstacle and the energy-supply region, the distribution of gasdynamic parameters obtained in the first stage for this distance is specified at the left-hand boundary of the calculation region. This approach permits considerable savings in machine time.

The gas motion in the calculation region is described by Euler and energy equations in divergent form; terms taking account of heat conduction are omitted in the energy equation. The correctness of this assumption requires further investigation.

All the parameters are reduced to dimensionless form as follows: The pressure, density, internal energy, velocities, and linear dimensions are referred to $\rho_\infty U_\infty^2$, ρ_∞, U_∞^2, U_∞, and r_1, respectively. At the upper and right-hand boundaries of the calculation region, so-called soft boundary conditions are specified, i.e., the first derivatives of the corresponding parameters are taken to be zero; At the surface of the body and the symmetry axis, impenetrability conditions are adopted. The problem is solved in a formulation with constant boundary conditions by the Godunov method [5]. The position of the plane end relative to the end of the energy-supply region $\bar{X} = x/r_1$ varies from 4.1 to 13.9. The radius of the obstacle varies in the range $\bar{R} = R/r_1 = 1.5$-3.5 with a step of 0.5. The energy-supply region is of dimensions 1.6 × 1 in the axial and radial directions. The specific power supply remains constant in all the calculations.

In analyzing the results of numerical modeling, it must be remembered that the flux is divergent up to $\bar{X} \approx 10$, and converges to the axis when $\bar{X} > 10.5$. The form of the leading shock wave and the eddy structures which form is shown in Fig. 1 as a function of the distance $\bar{X}$ between the plane end ($\bar{R} = 2.0$) and the energy-supply region (the pressure discontinuity behind the leading shockwave at the periphery of the end is not shown in Fig. 1). A toroidal eddy and an isolated shock wave, the geometry of which depends strongly on the relative position of the obstacle and the energy-supply region, is formed in front of the plane end in all cases up to $\bar{X} \approx 14$.

As is evident from Figs. 1a, b, the usual flow patterns and form of the leading shock wave are not realized at all for small distances from the plane end ($\bar{X} = 4.1$, 5.8), when the nonuniformity of the incoming flow is localized within the transverse dimension of the obstacle; the eddy is shifted toward the edge of the end, and is small ($\bar{R}_{eddy} \approx 0.3\bar{R}$). The reasons for the appearance of this flow structure are evident on scrutinizing Fig. 2, which shows the distribution of the pressure coefficient over the radius of the plane end. In fact, if $\bar{X} = 4.1$ (Fig. 1a), the pressure coefficients at the critical point and at the connecting line are approximately the same, which facilitates the displacement of the return flow toward the edge of the end. With further increase in $\bar{X}$, the pressure difference increases on account of the faster pressure reduction at the critical point due to the dispersion of the incoming flow; this is associated with movement of the eddy toward the symmetry axis, increase in its size, and the establishment of flow patterns similar to those in [3, 4] (Fig. 1c-e). In addition, the formation of a λ-type leading discontinuity close to the symmetry axis (Fig. 1f) is possible due to the reversal of the incoming flow converging on the axis at sufficiently large distances from the energy-supply region ($\bar{X} = 13.5$). With further increase in $\bar{X}$, the eddy decreases in size and disappears; the flow structure approaches that corresponding to uniform gas flow. In accordance with change in flow structure

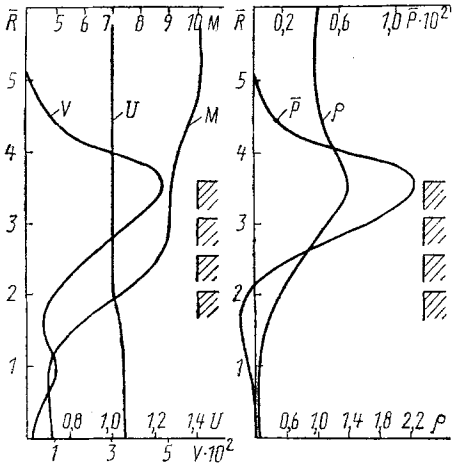

Fig. 4. Distribution of the gasdynamic parameters in the flow at a distance $\bar{X} = 9.1$ from the energy-supply region.

in the shock layer, the lateral-drag coefficient of the obstacle $C_{X\alpha}$ and the distance of the leading shock wave from the end change with increase in $\bar{X}$ (Fig. 3a). The greatest reduction in $C_{X\alpha}$ (by a factor of approximately 4.3) corresponds to the case of maximum distance of the leading shock wave from the plane end ($\bar{R} = 2$; $\bar{X} = 9.1$). At larger $\bar{X}$, the lateral-drag coefficient increases slightly, tending to a constant value which corresponds to M for the flow core, the uniformity of which increases with increase in $\bar{X}$.

The influence of the transverse directions of the obstacle on its lateral-drag coefficient may be seen in Fig. 3b, analysis of which yields the far-from-trivial conclusion that the lateral-drag coefficient of the plane end decreases by a factor of approximately 2.4 with increase in the radius $\bar{R}$ at constant $\bar{X} = 9.1$, reaching its smallest value in the given range of $\bar{R}$ ($2 \leq \bar{R} \leq 3.5$) at $\bar{R} = 3.5$ (continuous curve in Fig. 3b). However, when $\bar{R} \geq 2.5$, steady flow is not established, as indicated by the periodic oscillation of $C_{X\alpha}$. The oscillation amplitude of $C_{X\alpha}$ increases with increase in transverse dimensions of the obstacle $\bar{R}$ (dashed curves in Fig. 3b; the lower curve corresponds to the minimum value of $C_{X\alpha}$ and the upper curve to the maximum value). That such flow conditions may exist was suggested in [3].

Why nonsteady conditions appear may be understood if the radial distribution of the gasdynamic parameters in the flow arriving at the obstacle when $\bar{X} = 9.1$ is analyzed (Fig. 4). On the right-hand side of Fig. 4, the outer edges of plane ends of radii $\bar{R} = 2$, 2.5, 3.0, and 3.5 are shown to scale. It is evident from Fig. 4 that the maximum density, pressure, and transverse velocity correspond to the edge of the plane end with $\bar{R} = 3.5$. Considerable increase in pressure in the peripheral part of the end leads to the appearance of a powerful return flow similar to that in Fig. 1d, but of much greater extent. The leading shock wave then moves a distance $2.4\bar{R}$ away from the end, the slope of its lateral branches decreases, and the return flow becomes more intense. This leads to additional increase in the transverse velocity component; as a result, some of the high-pressure, high-density gas moves past the plane end, and the pressure in its peripheral region decreases, with consequent decrease in the intensity of the return flow and its extent along the axis. The leading shock wave moves closer to the obstacle and its slope increases, resulting in an increase in pressure at the outer edge of the end surface; then the process repeats itself.

This investigation shows that, in supersonic flow around a cylindrical obstacle with a plane front end, in the case of high axial nonuniformity of the gasdynamic parameters as a result of energy supply in a local region, three types of shockwave structure may exist, with steady and periodic flow conditions, and there is significant reduction in the lateral-drag coefficient; these characteristics are determined by the mutual position of the obstacle and the energy-supply region and by their relative dimensions.

NOTATION

R, obstacle radius; r_1, radius of energy-supply region; M, Mach number; Q, specific power supply; ρ, density; U, V, axial and radial components of the flow velocity; x, r, coordinates; $\bar{X}$, relative distance of the obstacle from the end of the energy-supply region; $\bar{R}$, relative radius of obstacle; $\bar{R}_{eddy}$, relative radius of eddy; $C_{X\alpha}$, lateral-drag coefficient of obstacle; $\bar{P}$, pressure coefficient. Indices: ∞, parameters of unperturbed flow.

LITERATURE CITED

1. I. A. Belov, Interaction of Nonuniform Flow with Boundaries [in Russian], Leningrad (1983).
2. N. D. Kovalenko, Perturbation of Supersonic Flow with Mass and Heat Supply [in Russian], Kiev (1980).
3. V. I. Artem'ev, V. I. Bergel'son, I. V. Nemchinov, et al., Izv. Akad. Nauk SSSR, Mekh. Zhidk. Gaza, No. 5, 146-151 (1989).
4. P. Yu. Georgievskii and V. A. Levin, Pis'ma Zh. Tekh. Fiz., 14, No. 8, 684-687 (1988).
5. S. K. Godunov (ed.), Numerical Solution of Multidimensional Gasdynamic Problems [in Russian], Moscow (1976).

INVERSE CASCADE IN FRACTAL TURBULENCE (VORTEX-FRACTONS)

A. G. Bershadskii*

UDC 532.517.4

A direct connection between the properties of the inverse cascade of energy and the fractal properties of turbulence is established.

Introduction. The transport of energy from small-scale to large-scale motions attracted attention long ago. A large body of literature is devoted to this topic (see, for example, [1-6]), and it can be asserted that its existence has been reliably established by experiment. It is considered that the inverse cascade is a characteristic feature of large-scale processes in quasi-two-dimensional turbulence. However, the physical nature of the inverse energy cascade is still not well understood, and there is a great deal of experimental material, obviously connected with the inverse cascade, which needs interpretation. Evidently, one of the fundamental points that is unclear here is the connection between the inverse cascade and the fractal character of turbulence. The difficulty in the theoretical analysis of this problem is due to the specific fractal structure in two-dimensional turbulence (for example, see [5, 7]). Below it will be shown that with the suppression of the fractal character of the motion, the inverse energy cascade in two-dimensional turbulence is also suppressed at large scales. That is to say, the very existence of the cascade turns out to be caused by the fractal character of the turbulence.

The carriers of the inverse cascade are the large-scale, localized fractal formations, closely linked to the fracton dimension of the fractal processes [8]. Evidently, the characteristic quasi-horizontal vortices with structures on the scale of ~1-100 km, which have been observed in the ocean [9], are such vortex-fractons (see below). In magnetohydrodynamic turbulence, it is still not possible to visualize vortex-fractons. However, the spectral and integrated characteristics of the processes, for which these vortices are responsible, have been measured in numerous experiments. Below, a comparison with these data will be made. This comparison indicates that for both the oceanic turbulence and the MHD turbulence, the inverse energy transfer to large scales is linked to processes of a fracton nature. A connection is established between the fracton dimension of the turbulence D_f [8] in the two-dimensional case and the low-frequency scaling spectrum of the kinetic energy of pulsation

$$E(\omega) \sim \omega^{D_f - 3}. \quad (1)$$

For the universal (approximate) value $D_f = 4/3$ [8] (Alexander–Orbach), relation (1) gives

$$E(\omega) \sim \omega^{-5/3}, \quad (2)$$

*Deceased.

Makeevskii Institute of Civil Engineering. Translated from Inzhenerno-fizicheskii Zhurnal, Vol. 62, No. 2, pp. 248-253, February, 1992. Original article submitted August 21, 1990.

 1062-0125/92/6202-0182$12.50